THE ASTRONOMICAL JOURNAL, 115:855–867, 1998 February


# THE SOUTHERN PROPER MOTION PROGRAM. I. MAGNITUDE EQUATION CORRECTION

TERRENCE M. GIRARD, IMANTS PLATAIS, VERA KOZHURINA-PLATAIS, AND WILLIAM F. VAN ALTENA
Department of Astronomy, Yale University, P.O. Box 208101, New Haven, CT 06520-8101

AND

CARLOS E. LÓPEZ
Universidad de San Juan and Yale Southern Observatory, Av. Benavídez 8175 Oeste, Chimbas, 5413 San Juan, Argentina
*Received 1997 June 16; revised 1997 September 15*

## ABSTRACT

As with virtually all photographic plate material, the astrograph plates from which the Southern Proper Motion (SPM) catalog is being compiled suffer from magnitude-dependent systematic shifts in the image positions, i.e., a magnitude equation. If left uncorrected, these would adversely affect both the primary goals of the SPM catalog, the absolute proper motions, and the faint secondary reference frame. Using the diffraction-grating images present on the plates, a procedure is adopted that allows a spatially variant magnitude equation correction to be derived individually for each SPM plate. Application of the method to $\sim 120$ SPM fields, primarily around the south Galactic pole and the $-30°$ and $-35°$ declination zones, demonstrates its effectiveness. Indeed, the method proves superior, in the case of the SPM, to a direct calibration of the magnitude equation using the newly available Tycho Catalogue. The result of the diffraction-grating technique is final SPM positions and proper motions that are largely magnitude equation–free, as verified by numerous internal and external checks.

*Key words:* astrometry — methods: data analysis

## 1. INTRODUCTION

The Yale/San Juan Southern Proper Motion (SPM) Program is the southern-sky complement to the Lick Northern Proper Motion Program (Klemola, Jones, & Hanson 1987). The SPM Program will produce absolute proper motions, positions, and $BV$ photographic photometry for approximately one million stars south of $\delta = -17°$. The proper motions are measured relative to external galaxies, and the positions will be on the International Celestial Reference System via the *Hipparcos* and Tycho Catalogues (ESA 1997). Program stars cover the magnitude range $5 < V < 18$, the majority of which are faint anonymous stars randomly selected for the purpose of studying Galactic kinematics. A more complete discussion of the SPM Program, including a description of the input star selection, can be found in Platais et al. (1992, 1993).

To date, 30 fields ($\sim 700$ deg$^2$) surrounding the south Galactic pole (SGP) have been measured and reduced. An additional $\sim 90$ fields, primarily in the $-30°$ and $-35°$ declination zones, have also been completed. Preliminary tests indicate the precision of the derived proper motions ranges from 1 to 4 mas yr$^{-1}$, depending on the number of measurable images per individual star. The uncertainty in the correction to absolute proper motion is approximately 1 mas yr$^{-1}$ per field. A complete discussion of the SGP results, along with additional details of the reduction procedures, is currently in preparation (Platais et al. 1998a). Here we present the technique used to ensure that the proper-motion accuracy just quoted is not undermined by magnitude-related systematics in the plate material.

Astrometric magnitude equations, i.e., shifts in an image centroid as a function of stellar magnitude, result from the combination of the nonlinear response of photographic emulsions and asymmetric image profiles. The asymmetry may be due to imperfections in the optical system, to polar misalignment of the telescope (field rotation), or to inexact guiding during the exposure. Each of these will introduce a magnitude equation into the image positions and, to the extent that the effect changes over time, will also affect the derived proper motions. We note that a magnitude equation can also be introduced during the plate measurement process, although modern measuring devices such as PDS microdensitometers will not do so when properly used.

Whatever its cause, the net result is photographic density profiles that are skewed; the degree of skewness increases in severity for the more heavily exposed images, i.e., for brighter stars. This causes a systematic shift between the image centers of stars of different brightnesses. In general, the form of the magnitude equation can also be position-dependent, varying across the plate. Three different strategies can be imagined for dealing with a magnitude equation: (1) avoiding it by choosing reference and target images of similar brightnesses (which may require artificially reducing the target image, as is commonly done in photographic parallax work), (2) calibrating the effect using additional external information, for instance, that members of a cluster share a common proper motion, or (3) deriving the offsets directly from multiple images of the same star with different effective magnitudes such as those created by use of an objective grating. The first of these is not an option for the SPM Program, since the program's very goal is to obtain proper motions and positions for a wide range of stellar magnitudes. The second can be used to correct the proper motions in those fields that contain clusters, but this is a limited number of fields, and the correction could still not be trusted over the entire extent of those fields. Besides, we also wish to derive *positions* that are free of magnitude equation, in particular for stars much fainter than the *Hipparcos*/Tycho reference stars. The third approach has been explored by Schlesinger & Hudson (1914), using multiple-offset exposures, and by Eichhorn (1956), using grating images. We adopt the formalism of Jefferys (1962), which we briefly reproduce in § 3 for convenience. This approach assumes that the central-order and first-order grating images are similar in form or, more precisely, that they share the same functional dependence of image center

on effective magnitude. While this will only be approximately true, the method is powerful in that it allows the magnitude equation to be derived internally for each plate and as a function of position across the plate. This is the technique used in the SPM reductions.

We note that with the recent release of the superb *Hipparcos* and Tycho astrometric catalogs, an alternative means of magnitude equation calibration presents itself, namely, direct calibration into an existing catalog reputed to be essentially without magnitude equation, i.e., *Hipparcos*/Tycho. Unfortunately, the limited magnitude range and, to a lesser extent, the spatial density of these catalogs combine to make them substantially less effective as magnitude equation calibrators for the purpose of the SPM program than the method described here.

In § 2, we describe the SPM plate material, which includes multiple images per star and an overview of how these images are used to link bright stars to faint stars and galaxies. In § 3, we provide details of our use of Jefferys's (1962) formulation to "bootstrap" the magnitude equation correction. In § 4, the method is applied to actual SPM plate measures and the validity of the results is checked by internal and external comparisons. A brief discussion of the advantage of the method, in the case of the SPM, over a direct calibration into the Tycho Catalogue is presented in § 5. In § 6, we conclude with some thoughts on the importance of magnitude equation correction and the potential of the SPM data as they relate to other large astrometric surveys currently underway.

## 2. PROGRAM OVERVIEW

### 2.1. *Plate Material*

The SPM plates are taken using the 51 cm double astrograph of Cesco Observatory in El Leoncito, Argentina. The plates, with a scale of $55''.1$ mm$^{-1}$, cover an area of $6^{\circ}.3 \times 6^{\circ}.3$ and are taken on 5° centers. Blue-passband (103a-O unfiltered) and visual-passband (103a-G with OG515) plates are obtained simultaneously. An objective grating, with grating constant $\Delta m = 3.85$, is used to produce measurable diffraction images through second order. Each plate contains two exposures, one 2 hr in duration and an offset exposure 2 minutes long which, combined with the grating, provide measurable images of stars and galaxies in the approximate range $5 < V < 18$ and $6 < B < 19$. For stars fainter than $V \sim 14$, only the long-exposure, central-order image is present. The first-epoch survey, which consists of 717 fields with very nearly full coverage south of $\delta = -17°$, was obtained in the years 1966–1974. The second-epoch observations commenced in 1987 and are still underway, with approximately one-third of the fields completed. Unfortunately, the discontinuation of the 103a emulsions by Kodak jeopardizes the completion of the second epoch. Suitable alternatives for the remaining second-epoch fields are being explored.

Some details of the plate material are noteworthy as they relate to the subject of the magnitude equation. The astrograph lenses have been suspected of suffering from lens decentering of at least one element (Platais et al. 1995), which introduces a field-independent coma. In addition to this, the long, fork mounting of the astrograph makes stable polar alignment difficult, resulting in field rotation. Also, the technique for guiding the long exposure has changed over the years. During the first-epoch observations, guiding corrections were made manually by updating the telescope pointing. For the second-epoch plates, guiding is facilitated by an image-dissector autoguider controlling stepping motors that reposition the plateholder. Throughout both epochs, all plates have been developed by hand. The combination of all of these elements leads to a large range in plate quality. Some plates suffer from slightly elongated images whose shape and orientation vary across the plate, an effect that is generally more noticeable on the visual plates, which have images sharper than the wider passband blue plates.

### 2.2. *Plate Measurement*

The plates are scanned with the Yale PDS microdensitometer, which has laser-interferometer metrology and submicron measuring precision—more than adequate for the moderately large-grained 103a emulsions. Time constraints do not allow the digitization of the full plates; instead, an input catalog is prepared and the program stars and galaxies are scanned in an object-by-object mode. Details of the input catalog preparation are given by Platais et al. (1992, 1993). Measurable grating images through second order are scanned and centered using a two-dimensional Gaussian fit to the density profiles (Lee & van Altena 1983). The centering program yields $(X, Y)$-positions, uncertainties in the positions and an instrumental magnitude for each image scanned. Stars and galaxies are centered with the same routine. A set of five "drift" stars is also repeatedly measured throughout the approximately 12 hr scan, and their measures are used to monitor and correct for drifts in the plate coordinate system due to thermal and mechanical relaxations in the PDS. Once drift-corrected, the positions are then precorrected for atmospheric refraction.

### 2.3. *Reduction*

Before either the proper-motion solution or the equatorial coordinate solution can be made, measures from the various grating and exposure systems must be combined into a single system on each plate. We adopt as a standard the system of the central-order images in the long exposure. First, the diffraction-grating image measures—actually, the mean positions of the first- and second-order pairs—are transformed to the system of the central order. This is the crucial step during which the magnitude-dependent effects are derived and corrected, as detailed in the procedure presented in § 3. This is done separately for the short and long exposures, using all available stars for which both central- and first-order images are measurable. Following this, the short-exposure positions are transformed to the long-exposure system using (as high as) cubic polynomial field terms derived from "bridge" stars—stars for which long-exposure first-order images and short-exposure central-order images are measurable. In this manner, positions of the bright stars are put on the same system as those of the faint stars and galaxies that will define the proper-motion solution.

Relative proper motions are derived by applying a least-squares–determined cubic transformation of the first-epoch measures into the system of the second-epoch measures. Faint anonymous stars, from 800 to 1300 per field, are used to calculate the transformation. The centering-error–weighted mean of the relative proper motions of external galaxies is then used to make a correction to absolute proper motion. This two-step process is necessary because

the sparsity and poor centering precision of galaxies on the SPM plates precludes their being used directly to derive the differential plate model.

Currently, the mean-epoch positions are transformed to celestial coordinates using cubic field terms and reference stars from the Catalogue of Positions and Proper Motions (PPM; see Bastian, Roeser, & Yagudin 1993). The absolute proper motions are also aligned to the celestial coordinate system during this transformation. Now that the *Hipparcos*/Tycho catalog is available, it replaces the PPM as our choice for reference system. Thus, all published SPM positions will be on the *Hipparcos*/Tycho system.

Parallel with the astrometric reductions, the instrumental magnitudes are calibrated to $V$ and $B$ in a two-step procedure. First, the differences in instrumental magnitudes of central and first-order grating images are used to "linearize" these magnitudes by forcing the differences to equal the known grating constant. The formalism of this linearization is mathematically similar to that of the astrometric magnitude equation and thus is also presented in § 3 for completeness. Once linearized, the final calibration of the magnitudes amounts to a constant offset which, in general, has a spatial dependence across the plate. This offset function is derived using a combination of CCD calibration photometry in one small area of the field along with $VB$ values extracted from the SIMBAD database of stars across the field. (With the newly available Tycho photometric data, we expect these stars to replace the SIMBAD stars as bright photometric calibrators for all SPM fields.) In practice, a linear and possibly small quadratic term in the linearized instrumental magnitude is also needed, in addition to the purely geometric terms.

## 3. MAGNITUDE EQUATION CORRECTION

The method we use for deriving the magnitude equation corrections is that laid out by Jefferys (1962), who in turn credits Eichhorn (1956) for the first arithmetic use of this general procedure. The basic approach is as follows: Assume the magnitude equation produces offsets in the image positions of the form

$$\Delta X = F(m, X, Y) , \quad \Delta Y = G(m, X, Y) , \tag{1}$$

which is Jefferys's equation (1), where $m$ is the effective magnitude of an image and $(X, Y)$ is its position on the plate. While the offset for any single image is not known, the difference in offsets of two images of the same star can be measured and will be nonzero if there is a difference in the "effective" magnitude of the two images, as with central and first-order grating images, for example. We assume that in the absence of magnitude-dependent offsets, the mean position of the diffraction-grating pair would coincide with the position of the central-order image and that the form of the magnitude equation, $[F(m, X, Y), G(m, X, Y)]$, is identical for the central and diffracted images. Presumably, the latter assumption will only be approximately true, and more so for the first-order images as opposed to higher order images. To the extent that it does hold, the difference between the central-image position, $(X_0, Y_0)$, and the mean position of the $i$th-order pair of images, $(X_i, Y_i)$, will be

$$\begin{aligned} X_i - X_0 &= F(m_i, X_0, Y_0) - F(m_0, X_0, Y_0) , \\ Y_i - Y_0 &= G(m_i, X_0, Y_0) - G(m_0, X_0, Y_0) , \end{aligned} \tag{2}$$

which is Jefferys's equation (3), where $m_0$ and $m_i$ are the effective magnitudes of the central- and $i$th-order images, respectively. Choosing an appropriate form for the functions $F$ and $G$ with coefficients $f_n$ and $g_n$, the coefficients can be determined by a least-squares solution using a sufficient number of stars for which both the central and grating images can be measured.

In practice, we find that describing the magnitude equation present in the SPM plate material requires a rather large number of polynomial terms in some cases. We use the following general functional forms:

$$\begin{aligned} F = {} & f_1 m + f_2 m^2 + f_3 m^3 + f_4 mX + f_5 mY + f_6 mX^2 \\ & + f_7 mXY + f_8 mY^2 + f_9 mX^3 + f_{10} X^2 Y \\ & + f_{11} m^2 X + f_{12} m^2 Y , \\ G = {} & g_1 m + g_2 m^2 + g_3 m^3 + g_4 mY + g_5 mX + g_6 mY^2 \\ & + g_7 mXY + g_8 mX^2 + g_9 mY^3 + g_{10} Y^2 X \\ & + g_{11} m^2 Y + g_{12} m^2 X . \end{aligned} \tag{3}$$

Note that the coefficients $f_n$ and $g_n$ can be found by using differences between the central- and first-order image positions or those of central- and second-order images, i.e., $i = 1$ or $i = 2$ in equation (2). Jefferys (1962) found that the first- and second-order solutions yielded very different coefficients on the McCormick 26 inch (0.66 m) refractor plates of his study. We find that this is not the case with the SPM plate material. The first- and second-order images yield similar solutions. Thus, we have chosen to use the first-order images to derive the magnitude equation correction, and this is applied to all measured images, central through second order. On the other hand, the long-exposure and short-exposure magnitude equations are found to be significantly different, and therefore these two corrections are derived separately.

Interpretation of the coefficients in equation (3) is simplified by using properly linearized magnitudes, but with the zero point set near the plate limit. The raw, instrumental magnitude estimates produced by the centering software are not properly scaled or even linear with true apparent magnitude. Thus, the first half of the photometric calibration described in the previous section is performed prior to the solution for the $(f_n, g_n)$ in order to provide the necessary magnitude values. This linearization of the instrumental magnitudes also utilizes differences between the central- and first-order image parameters, in this case, differences in the photometric parameter.

Assume that the "proper" magnitude estimates, $m$, are some function of the raw instrumental magnitudes, $p$, along with a possible field dependence:

$$m = H(p, X, Y) . \tag{4}$$

The difference between the first-order and central-image magnitudes, $m_1$ and $m_0$, will simply be the grating constant, $\Delta_g$, which is taken to be 3.85, the approximate value for the SPM gratings. Thus,

$$\Delta_g = H(p_1, X_0, Y_0) - H(p_0, X_0, Y_0) , \tag{5}$$

where, as with equation (2), the $(X, Y)$-position may be represented by the central-image position without any loss of accuracy. The functional form adopted for $H$ is

$$\begin{aligned} H = {} & h_1 p + h_2 p^2 + h_3 p^3 + h_4 p^4 + h_5 p^5 + h_6 pX \\ & + h_7 pY + h_8 pX^2 + h_9 pXY + h_{10} pY^2 . \end{aligned} \tag{6}$$

As before, all stars on the plate for which central- and first-order images can be measured are used to solve for the coefficients $h_n$ by least-squares solution. Once determined, the function $H$ is applied to all images, central through second order. (The high degree of the polynomial in $p$ is not particularly troublesome, as extrapolations are slight and infrequent.) Separate solutions are made in the short and long exposures, and a final offset is applied to set $m = 0$ near the plate limit. This is primarily to simplify interpretation of the derived magnitude equation corrections, forcing them to equal zero at the plate limit.

## 4. APPLICATION

### 4.1. *Practical Aspects*

The degree to which the magnitude equation affects the SPM plates is suggested by Figure 1. The precorrection differences in position between the long-exposure central-order image and the mean of the first-order images are shown for a typical, blue-passband, second-epoch plate. A linear magnitude equation on the plate would show itself as a constant, nonzero offset in these difference plots. A quadratic magnitude equation would produce a slope in the ($\Delta X$, $\Delta Y$) versus magnitude plots. And a coma term, i.e., magnitude times coordinate, would produce a slope in the $\Delta X$ versus $X$ and $\Delta Y$ versus $Y$ plots. It can be seen from Figure 1 that this plate suffers from a significant coma-like effect in both coordinates and a quadratic magnitude equation in $Y$.

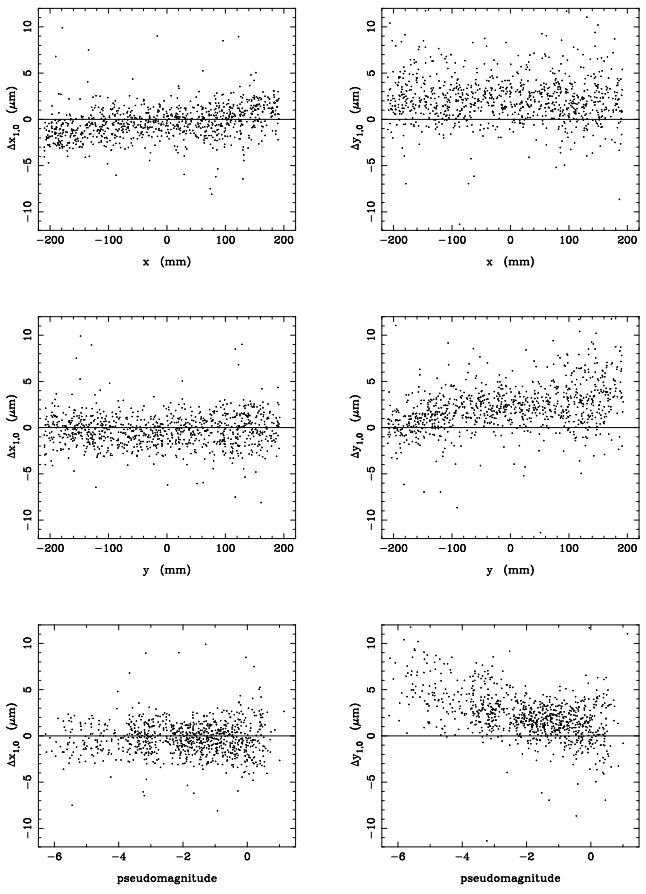


FIG. 1.—Positional differences between central and first-order grating images in the long-exposure system of a typical second-epoch blue plate (No. 384) as a function of plate coordinate and image magnitude. The effective magnitude difference between the central and first-order grating images is 3.85 mag. The pseudomagnitudes plotted in the bottom panels are essentially $B$ magnitudes with an arbitrary zero point.

This plate's values of the coefficients for linear magnitude equation and coma lie in the middle of the distribution for second-epoch blue (B2) plates. Figures 2 and 3 show the distributions of the dominant linear terms in equation (3) (terms $f_1, f_4, g_1, g_4$) for the long-exposure systems of the SPM plates reduced thus far. Actually, the B2 plates are the best behaved group in this respect, showing a relatively tight grouping in both figures. The V2 plates, on the other hand, display the widest range of values. The field-to-field variation of the coefficients within each group is quite significant, as can be judged from the scatter relative to the formal errors of the coefficients, which are slightly smaller than the size of the symbols plotted. (This intrinsic variation precludes a possible "stacking" of the plate residuals to better determine the coefficients.) The $X$- and $Y$-components of the coma are highly correlated but generally do differ significantly, and thus the simpler form of a radial coma was not assumed. Most worrisome is the fact that the mean values, and that of the coma in particular, differ between the first and the second epoch. If left uncorrected, or merely undercorrected, this could lead to survey-wide systematic effects in the derived proper motions.

In fact, such an effect was detected during a comparison with *Hipparcos* proper-motion data. These data covered 63 SPM fields and were made available to us for the purpose of helping to determine the link of the *Hipparcos* proper motions to the extragalactic reference system (Lindegren & Kovalevsky 1995; Platais et al. 1998b). Figure 4 shows the correlation between the per field mean proper motion differences, *Hipparcos* minus preliminary SPM, and the amount of magnitude equation correction applied to the SPM data. The SPM proper motions plotted in Figure 4 are the weighted average of all six exposure/grating-image systems from the visual SPM plates, although for the relatively bright *Hipparcos* stars, the central-order, long-exposure image receives very low weight. The weights are based on the scatter of each image system about the mean of the others for all stars measured.

The sign of the correlation observed in Figure 4 indicates that the SPM data have been *overcorrected* for magnitude equation. A similar effect is observed in the blue plates. Significantly, though, the various image systems yield consistent results, i.e., the central-order, long-exposure–derived proper motions have the same offsets from the *Hipparcos* data as do the first-order, short-exposure proper motions, which are based on images fainter by nearly 8 mag. This implies that the stellar images are indeed being corrected properly, but that the corrections to absolute proper motion, which are based on the measured "reflex" motions of the galaxies, are to blame. Further evidence that the zero-point corrections are correlated with the amount of magnitude equation correction is seen in Figure 5. Here the difference in zero-point correction, blue minus visual plates, are plotted as a function of the difference, blue minus visual, of the differences in linear magnitude equation correction, second epoch minus first. Although noisier than the data in Figure 4, a similar correlation is evident.

Two possible causes for this residual magnitude equation in the zero-point corrections have been postulated: (1) the polynomial adopted for the magnitude equation (i.e., eq. [3]), combined with the disparity in measuring precision between bright and faint images could lead to a poor repre-

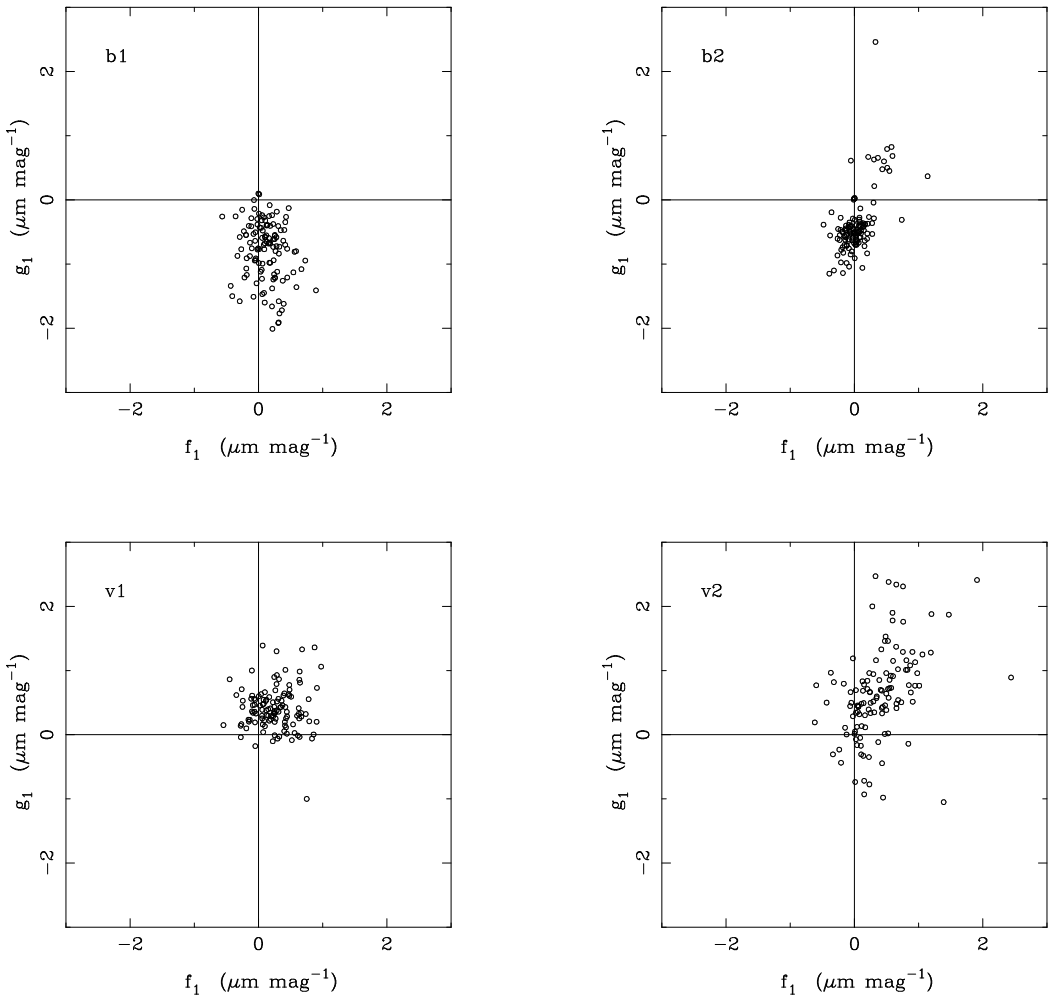


FIG. 2.—Distribution of linear magnitude coefficients ($f_1$ vs. $g_1$ in eq. [3]) for the approximately 120 SPM fields reduced thus far. The top panels show the first- and second-epoch blue plates, while the bottom panels show the first- and second-epoch visual plates. The typical error in the coefficients, as estimated from the least-squares reduction, is 0.02 $\mu$m mag$^{-1}$, roughly one-fourth the diameter of the plot symbols. Clearly, the field-to-field variation in the coefficients is real.

sentation at the faint end, and in particular, the region occupied by galaxies, and (2) the galaxies may be subject to a magnitude equation that is significantly different from that affecting the stellar images.

As for the first hypothesis, our experience with a number of open cluster proper-motion studies (e.g., Kozhurina-Platais et al. 1995; Dinescu et al. 1996) has indicated that neither a linear nor a quadratic polynomial provides a good description of a guiding-error–induced magnitude equation. One would expect that as one approaches the faint plate limit, the magnitude equation should flatten out. We have experimented with a modified version of equation (3) that was constrained such that the derivative with respect to magnitude was forced to zero at a magnitude $\delta m$ above the plate limit and continues flat to the limit. All SPM fields were rereduced using ever-increasing values of $\delta m$ until a plot equivalent to Figure 5 no longer showed a significant trend. The necessary value of $\delta m = 2.5$ mag, however, resulted in much poorer final proper motions as judged by a comparison between different image orders, as well as in direct comparison with *Hipparcos* data. This approach was therefore rejected.

The second hypothesis, that the galaxies are subject to a different magnitude equation than are the stars, is problematic. The individual measuring precision of the galaxy proper motions is much too poor to allow us to detect, let alone calibrate, the magnitude equation of the galaxies directly for any given field. Instead, we make the (hopeful) assumption that the galaxy images behave differently from those of the stars in a consistent way from field to field and use the ensemble of all measured fields to derive a correction to the zero points. This is probably not an unreasonable assumption. The mean difference in image shapes between stars and galaxies is roughly consistent from field to field; at least, it is always in the same sense (i.e., galaxies are always broader), although the difference is greater on the visual plates. Presumably, the different behavior of the galaxy images is due to their being broader than the stellar images, causing the onset of the magnitude equation to occur at a different magnitude. Therefore, we adopt as the form of the galaxy magnitude equation correction one that is the same as that of the stars but evaluated at a magnitude equal to that derived for the galaxy plus $\Delta m_g$. The value of $\Delta m_g$ will be chosen so as to minimize the slopes observed in Figures 4 and 5.

Actually, with a proper conversion of units the slope in

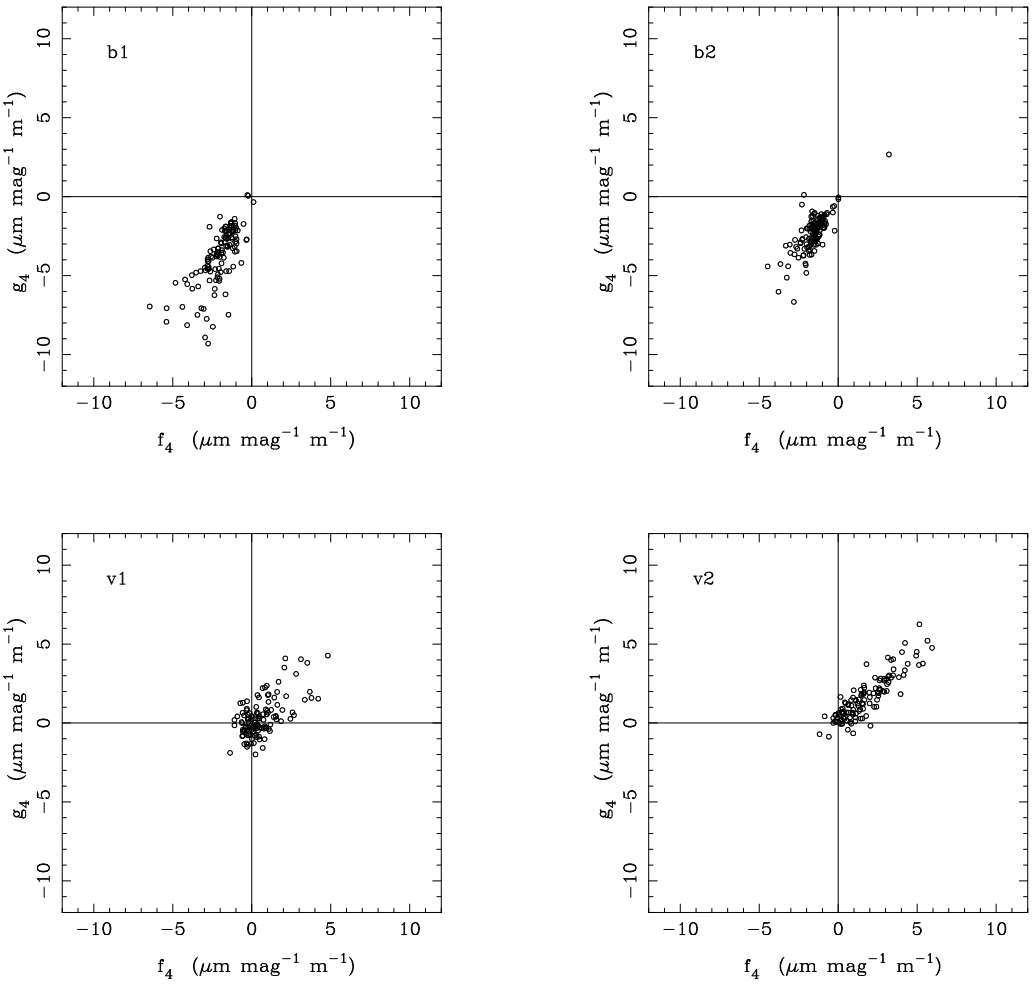


FIG. 3.—Distribution of "coma" coefficients (terms $f_4$ vs. $g_4$ in eq. [3]), for the same SPM plates as in Fig. 2. The plates are again grouped by blue and visual passbands and by first and second epochs. The typical formal error of the coefficients is 0.15 $\mu$m mag$^{-1}$ m$^{-1}$, roughly half the diameter of the plot symbols. The units given for the coma are such that the values may be best appreciated by keeping in mind that the SPM plates are roughly 0.4 m per side.

Figure 5 is exactly the desired magnitude offset. The mean of the slopes in $X$ and $Y$ yields $\Delta m_g = -0.7$ mag. In other words, the galaxies suffer from the same magnitude equation as stars that are 0.7 mag brighter. This is contrary to our expectation that the broader galactic images would be *less* susceptible to magnitude equation effects. Possibly the answer lies in the magnitude calibration itself, which is based entirely on stellar images and perhaps underestimates the brightness of galaxies (see, e.g., Fig. 3 of Platais et al. 1993). It could also be that this shift approximates some other underlying cause. We note that artificially brightening the galaxies reduces the magnitude difference between the galaxies and the mean of the anonymous reference stars upon which the proper-motion solution is based. Whatever its origin, we shall adopt the empirically determined value of $\Delta m_g = -0.7$ mag. Its positive effect on the proper-motion zero points is evident in Figures 6 and 7.

### 4.2. *Assessment*

After the magnitude equation corrections described above are made, the SPM proper motions and positions may be evaluated using both internal and external comparisons to search for remaining magnitude-dependent effects. Internal checks include comparing data derived from blue- and visual-plate pairs and also from the overlap regions of adjacent fields. Figure 8 shows the proper-motion differences, blue minus visual, from the central-order long-exposure images for a sample SGP field. The obvious trends in the uncorrected proper motions (*left*) are no longer present in the corrected data (*right*). It is important to note that the blue and visual plates are corrected totally independently of one another as regards magnitude equation. Thus, the agreement between blue- and visual-plate results provides confidence that each plate has been corrected properly. A similar improvement is achieved in the mean-epoch positions. While the corrections eliminate the trends with magnitude, a significant constant offset between blue and visual results is sometimes present in the proper motions, positions, or both. This is due primarily to the uncertainty in the correction to absolute proper motion for the proper motions and to plate-modeling error in the case of the positions. The manner in which these offsets are handled in combining the blue and visual data is discussed by Platais et al. (1998a).

The second type of internal check, employing the overlap region of adjacent fields, is demonstrated in Figure 9. The differences in derived declinations at the mean epoch for stars in common between the two fields' blue-plate pairs is

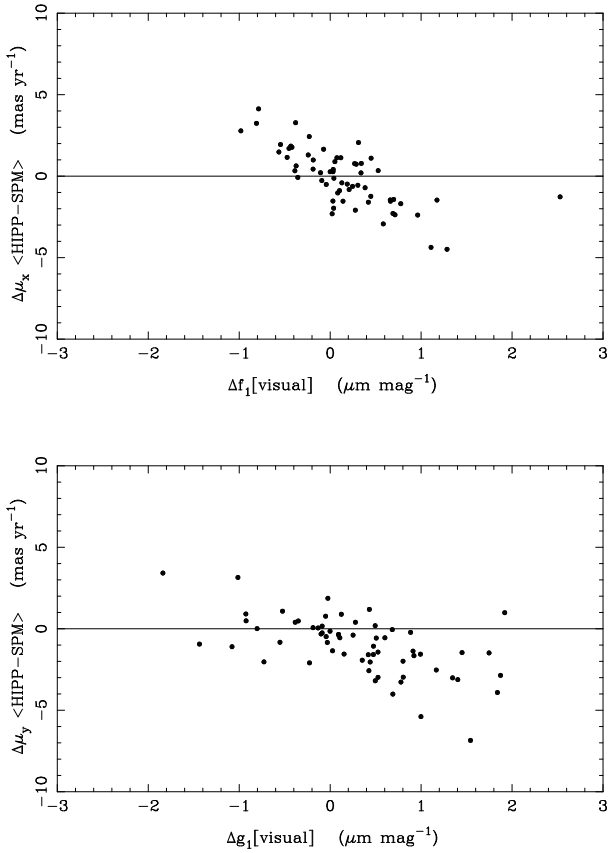


FIG. 4.—Proper-motion differences, *Hipparcos* minus preliminary SPM, as a function of the amount of magnitude equation correction applied during the SPM reductions (i.e., the difference between the magnitude equation term applied to the positions on the first- and second-epoch plates). Each symbol represents the mean of approximately 80–100 *Hipparcos* stars per field. The SPM proper motions are from the visual plates, although a similar trend exists for the blue plates.

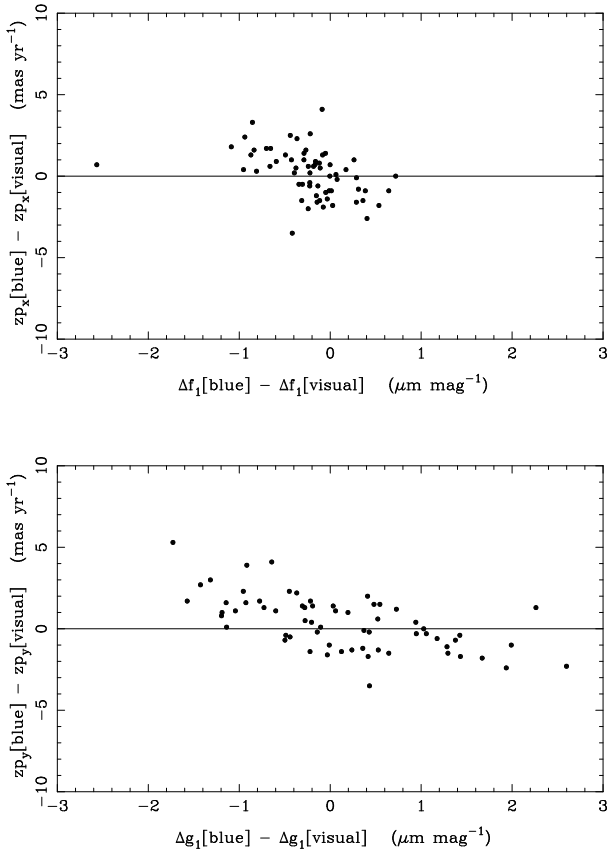


FIG. 5.—Differences, field by field, between the zero-point correction to absolute proper motion derived for the blue- and the visual-plate pairs during the preliminary SPM reductions. The zero-point correction is basically the proper motion difference between the galaxies and the mean of the reference stars used to perform the differential plate solution. These are plotted as a function of the differences, the blue plate minus the visual one, and second-epoch plate minus the first-epoch one, in the amount of magnitude equation correction applied to the individual SPM plates. The trend indicates that either the stars are being overcorrected or the galaxies are being undercorrected for magnitude equation.

shown both with and without magnitude equation corrections. The bottom panel, that with the corrections, still shows some slight residual structure as a function of magnitude. Note that, in the middle panel, in which one field is corrected and the other is not, the corrections are in fact quite large. The scatter of the final differences for stars with $B < 16$ is 0.″09, implying a precision of 0.″06 (1.1 $\mu$m) per field for a single passband and single image system.

The most important external check on the SPM data is comparison with *Hipparcos* proper motions and positions. The usefulness of the proper motions has already been illustrated in Figure 6 for those selected SPM fields for which we had access to preliminary *Hipparcos* data for the purpose of determining the proper-motion link. With the recent release of all *Hipparcos* data, we will be able to double the number of fields in a plot such as Figure 6 and, hopefully, verify the value for the galaxy magnitude offset discussed in § 4.1. The positions from *Hipparcos* also allow a direct comparison, and we were fortunate to be provided preliminary *Hipparcos* positions for a number of the SPM south Galactic pole fields. The $Y$-coordinates from a second-epoch blue plate of one such field are compared with *Hipparcos* positions in Figure 10. Although the magnitude range is limited, a magnitude equation is obvious in the uncorrected SPM positions and absent from the corrected data.

A second type of external check can be made on the SPM proper motions by isolating a sample of objects known to possess common proper motions, such as a star cluster. Figure 11 shows the SPM proper motions of tentative members of the open cluster Blanco 1. There is no detectable magnitude equation remaining in $\mu_x$ over the 9 mag spanned by the cluster sample. In $\mu_y$, which is typically the more afflicted of the two coordinates for the majority of the SPM plates, there is a slight residual trend with magnitude for the visual plates, approximately $-0.4$ mas yr$^{-1}$ mag$^{-1}$. This corresponds to 0.16 $\mu$m mag$^{-1}$, whereas the expected uncertainty, based on a propagation of the formal errors in the applied magnitude terms, is 0.08 $\mu$m mag$^{-1}$. Thus, the slope is only marginally larger than expected. The precision of the final SPM proper motions can be estimated from the scatter in Figure 11 about the mean motion of the cluster. The dispersion is 1.9 mas yr$^{-1}$ per plate pair in each coordinate. Note that the plates contributing to these proper motions were corrected with magnitude terms ranging from $-0.4$ to 1.0 $\mu$m mag$^{-1}$ and coma terms from $-3.5$ to 2.5 $\mu$m mag$^{-1}$ m$^{-1}$.

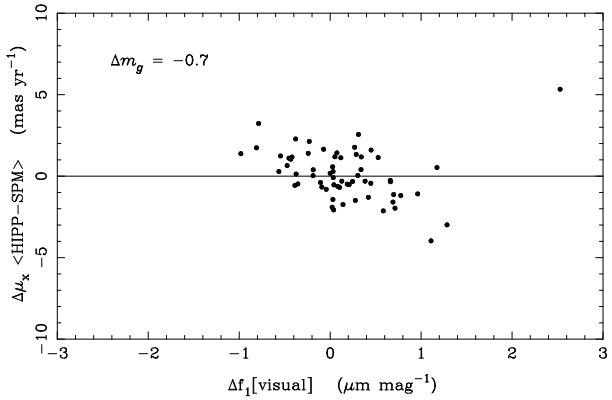


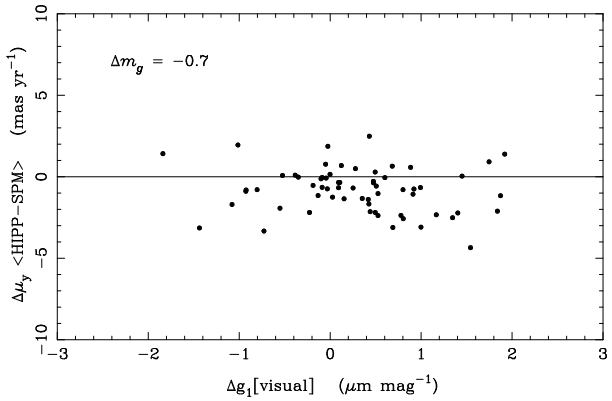


FIG. 6.—Same as Fig. 4, but after having modified the SPM zero-point corrections to absolute proper motion by making an adjustment of −0.7 mag in the galaxy image pseudomagnitudes as described in the text. There is definite overall improvement, although a residual trend in $\mu_x$ remains.

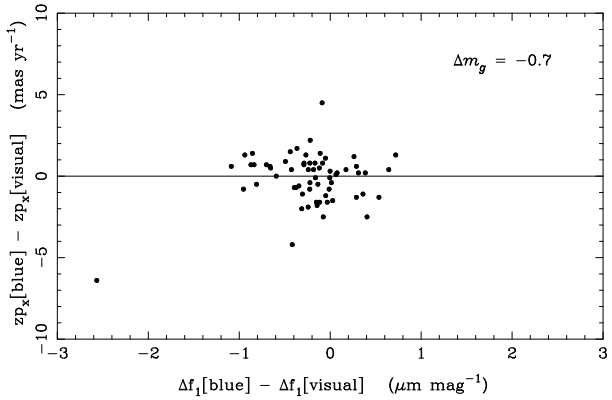


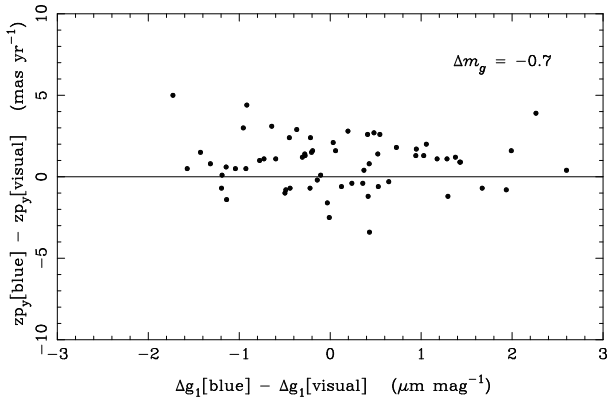


FIG. 7.—Same as Fig. 5, but after the adjustment of −0.7 mag to the galaxy pseudomagnitudes and the resulting changes in the zero-point corrections to absolute proper motion. The value of −0.7 mag was, in fact, chosen to minimize the slopes in these blue minus- visual difference plots. Note that the highly discordant point in the $\mu_x$ plot is due to a severely afflicted second-epoch visual plate, for which we may obtain a replacement.

## 5. COMPARISON WITH TYCHO-BASED CALIBRATION

It might be thought that the magnitude equation–free *Hipparcos*/Tycho catalog would provide a more direct and much more effective means of removing the magnitude-related systematics in the SPM plate material. Unfortunately, this is not the case. While, in the short-exposure system of the SPM, Tycho yields comparable results to the differential grating method we have adopted, such is not the case with the long-exposure system. This is primarily because of the limited magnitude range of the Tycho Catalogue, as we demonstrate below.

The *Hipparcos* Catalogue provides very accurate positions (∼1 mas) and proper motions (∼1 mas yr$^{-1}$) for approximately 100 stars per SPM field at roughly 11th magnitude and brighter. The Tycho Catalogue, which includes those *Hipparcos* data, is denser yet less accurate, providing approximately 440 stars per SPM field (in the SGP region) in a magnitude range similiar to *Hipparcos*, but with ∼25 mas positional accuracy at epoch 1991.25. All *Hipparcos* stars are included for measurement in the SPM program. The Tycho Catalogue is not explicitly included in the SPM program, however, since the SPM input catalog does include the PPM, the Southern Reference Stars, and the other relatively bright catalogs (see Platais et al. 1992, 1993 for a more complete description), we find that in the SGP region roughly 70% of the Tycho stars are also SPM program stars.

The measuring precision of a typical SPM stellar image is about 1 $\mu$m, or 55 mas. Both *Hipparcos* and Tycho positions are substantially better, and therefore we are limited (at least at the second epoch of SPM in the case of Tycho) by the SPM centering precision. Thus, despite the superior precision of *Hipparcos*, Tycho provides a better reference system for SPM calibration, as a consequence of its higher star density. As a test of the effectiveness of Tycho for calibration of the SPM magnitude equation, we have selected two second-epoch SPM plates and transformed their raw measures (i.e., uncorrected for magnitude equation) into the Tycho positions using a plate model that includes general quadratic magnitude terms. Separate calibrations were performed for the long and short exposures. In each solution, the central and first-, and second-order grating images were used simultaneously (weighting the average of a grating pair as a single image), with the properly scaled SPM magnitude estimates providing "effective" magnitudes for all images.

The results, as represented by the formal errors of the derived coefficients for the mag$^2$ terms, are listed in Table 1. For comparison, the mean formal errors of the corresponding terms from the standard SPM magnitude equation solution (terms $f_2$ and $g_2$ from eq. [3]), are also listed. In the short exposure, the two methods yield comparable accuracy on the visual plate, while the standard SPM solution performs marginally better on the blue plate. The numbers of

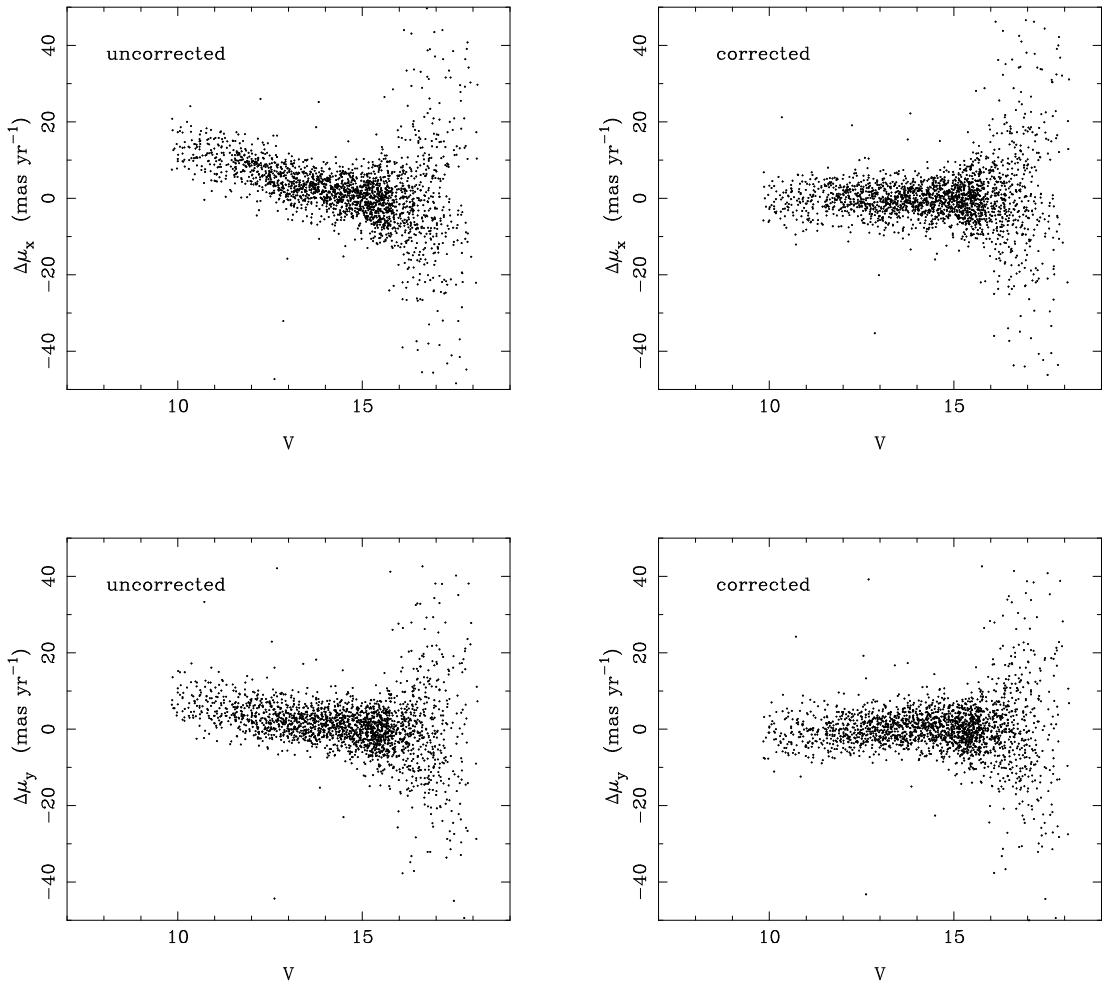


FIG. 8.—Differences in proper motions derived from blue plates and from visual plates for a sample SPM field (No. 457). Data displayed in the left panels have not been corrected for magnitude equation, while data in the right panles have been corrected.

stars contributing to the two solutions, $N_{st}$ in Table 1, are roughly equal on the blue plate, but the number of measurable Tycho stars on the yellow plate is significantly higher. The higher number is due to the relatively faint Tycho stars for which the short-exposure central-order image is measurable on the yellow plate but not the short-exposure grating images. These stars can contribute to the Tycho-based solution but not to the standard SPM solution, which is based on central/grating-order differences. On both plates, the number of reference images in the short-exposure solution, $N_{im}$, favors the Tycho solution, partly becuase of the inclusion of the second-order grating images. With a larger number of reference images, one would expect the Tycho-based solution to outperform the differential-grating method on the yellow plate in particular, yet it does not. This is possibly because of a correlation between the magnitude-dependent terms and the purely geometric terms in the plate model required of the Tycho-based solution. In

TABLE 1

COMPARISON OF MAGNITUDE EQUATION CORRECTION METHODS

| METHOD | SHORT EXPOSURE | | | | LONG EXPOSURE | | | |
|---|---|---|---|---|---|---|---|---|
| | $\sigma_x$ | $\sigma_y$ | $N_{st}$ | $N_{im}$ | $\sigma_x$ | $\sigma_y$ | $N_{st}$ | $N_{im}$ |
| Visual plate (598V2): | | | | | | | | |
| Tycho-based..... | 1.60 | 1.81 | 273 | 516 | 0.88 | 0.96 | 270 | 805 |
| Diffraction grating..... | 1.59 | 1.93 | 195 | 390 | 0.39 | 0.47 | 821 | 1642 |
| Blue plate (598B2): | | | | | | | | |
| Tycho-based..... | 1.16 | 1.12 | 275 | 751 | 1.97 | 1.93 | 148 | 443 |
| Diffraction grating..... | 0.86 | 0.87 | 268 | 536 | 0.28 | 0.30 | 945 | 1890 |

NOTE.—Quoted errors represent formal errors of mag$^2$ terms in mas mag$^{-2}$.

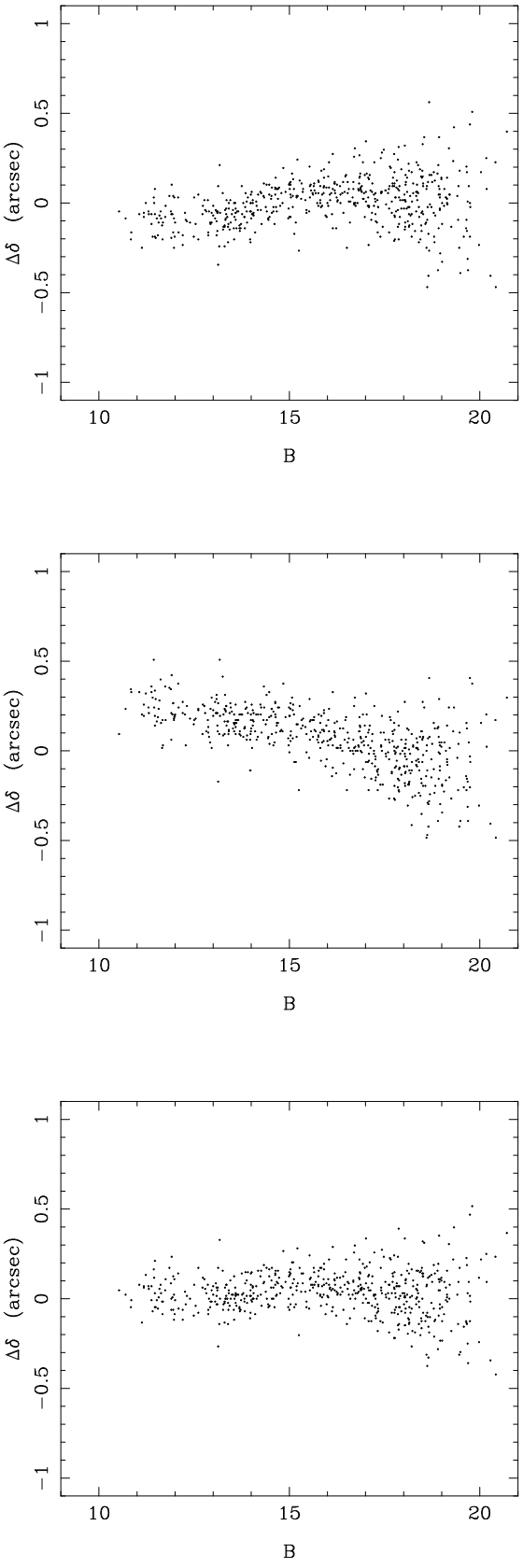


FIG. 9.—Differences in declinations derived for stars in the overlap region of two adjacent SPM fields (Nos. 385 and 386) as a function of *B* magnitude. The positions are at mean epoch of the blue-plate pairs in each field and based solely on the central-order, long-exposure image system. The top figure displays data not corrected for magnitude equation. In the middle panel, one field has been corrected and the other has not. In the bottom panel, both fields have been corrected.

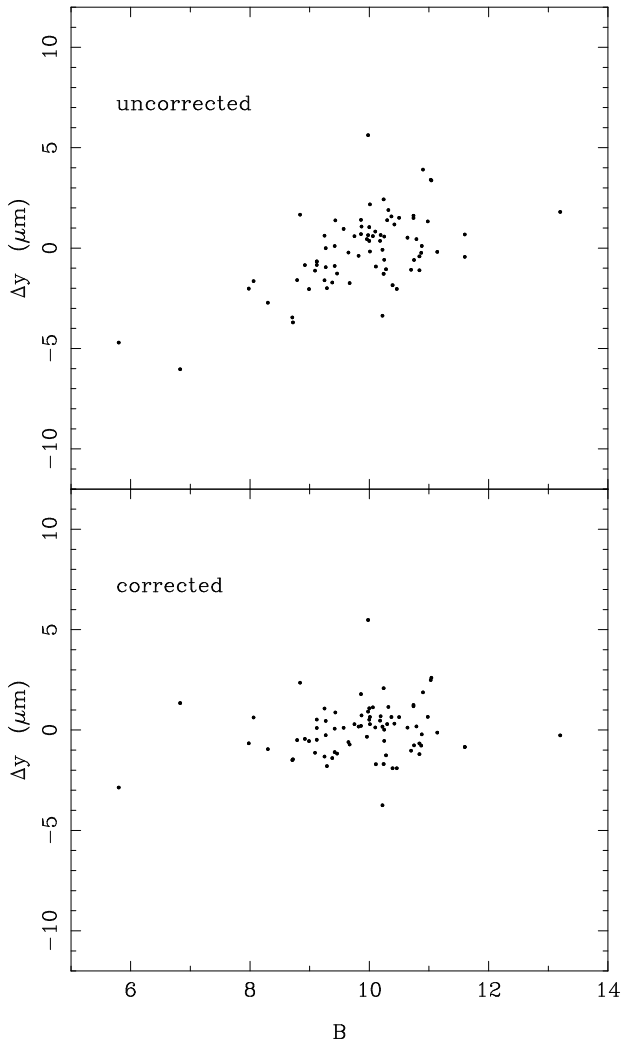


FIG. 10.—Differences in *Y* position, *Hipparcos* minus SPM, for a sample second-epoch blue plate (No. 526). The SPM positions are from the central-order, short-exposure images. The top and bottom panels are of SPM data before and after correction for magnitude equation, respectively.

the standard SPM method, only magnitude-dependent terms are involved.

In the long-exposure system, the Tycho-based solution yields much larger uncertainties, by factors of 2–6, relative to the standard SPM method. Not only are the formal errors of the solution larger, but the range in effective magnitude over which the terms are applicable is also reduced. This is illustrated in Figure 12, in which the distributions in effective magnitude for the two solutions are compared. In the short-exposure system, the two methods rely on roughly similar reference image distributions. In the long-exposure system, there are many more central- and first-order pairs measured, sampling a broader range in effective magnitude than Tycho alone can provide. It is this combination of greater numbers of images and their wider effective magnitude range that makes the adopted central/grating-order difference method superior to a direct Tycho-based magnitude equation calibration in the long-exposure system of the SPM plate material.

One could envision a procedure in which the Tycho-

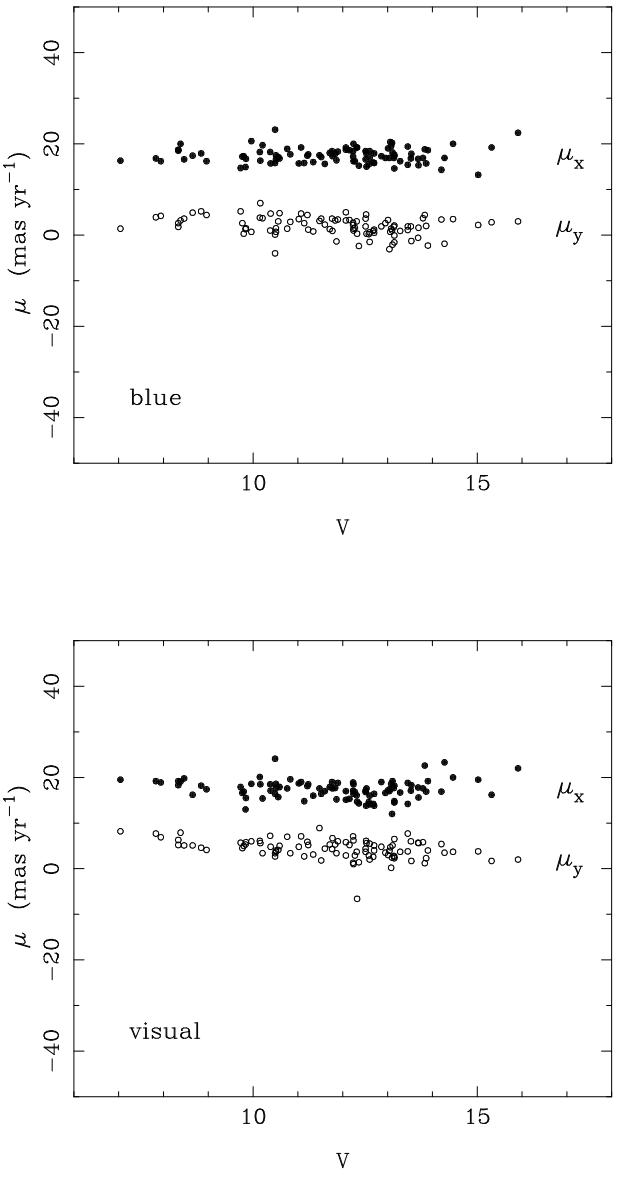


FIG. 11.—SPM-derived proper motions for tentative members of the open cluster Blanco 1. The top panel shows $\mu_x$ (*filled circles*) and $\mu_y$ (*open circles*) derived from the blue-plate pair and representing the weighted mean of the various image systems. The bottom panel shows the proper motions derived from the visual-plate pair. The scale of the plots matches that of Fig. 8 for the sake of comparison.

based solution is used to calibrate the short-exposure system and the central/grating-order difference method is used for the long exposure. However, there is no indication that the short-exposure calibration would benefit at all. In addition, a calibration based on Tycho/*Hipparcos* is problematic for the first-epoch SPM plates. It is our desire to keep the SPM absolute proper-motion system independent of the *Hipparcos* system. (Indeed, the *Hipparcos* proper-motion link to the extragalactic reference system is based, in part, on SPM data.) Even the use of proper motions derived from Tycho minus Astrographic Catalogue (AC) positions could introduce a bias from the *Hipparcos* system as, undoubtedly, the *Hipparcos* proper motions will be needed to correct the magnitude equation in the AC.

For these reasons, we feel that it is clearly best to adopt the central/grating-order technique for both the long and short exposures.

## 6. CONCLUSIONS

The plate material used in the SPM program, as is true of all plate material, suffers from varying degrees of magnitude equation. Making use of the positional differences in the central-order and diffraction-grating images, it is possible to derive individual corrections for each SPM plate. The resulting stellar positions and proper motions are free of significant magnitude effects, as shown by a number of checks made possible by the multiple image systems measured (i.e., long and short exposures, overlap regions, and blue and visual plates), as well as by direct comparison with external data such as the *Hipparcos* Catalogue.

Unfortunately, it is unlikely that many other photographic surveys are able to make direct use of the magnitude equation correction techniques discussed here, because of the requirement of having grating images or multiple exposures. While these other surveys will be able to use the *Hipparcos* and Tycho Catalogues to calibrate their magnitude equation down to a magnitude of approximately 11, extending the calibration to fainter magnitudes is crucial. We are fortunate in the case of the SPM to have an alternate method of calibration that allows correction down to the plate limit and on a plate-by-plate basis.

Final SPM positions and proper motions are presently available for 32,000 stars in an extended region around the south Galactic pole and spanning the magnitude range $5 < V < 18$. A complete description of these data is given by Platais et al. (1998a). Also nearing completion are the entire $-30°$ and $-35°$ zones (minus the fields containing the Galactic plane). These zones will be presented in the near future.

We feel that these SPM data present an invaluable resource for studies of Galactic structure. They also have the potential to be an important source of calibration for other, deep photographic surveys, primarily the numerous Schmidt-based programs now underway. While yielding vast numbers of absolute stellar proper motions, the usefulness of the Schmidt plate data may be undermined if significant systematics go undetected and uncorrected. Preliminary SPM data have contributed to the development of one technique for removing the geometric distortions inherent in Schmidt plate measures (Bucciarelli et al. 1995). While several such techniques now exist for treating the purely geometric distortions, the magnitude effects are potentially more troublesome. Morrison et al. (1996) have investigated the constant, repeatable component of magnitude equation in Schmidt plate measures, using overlap regions; however, the plate-to-plate variation of the magnitude equation remains largely unexplored. Lu et al. (1996) conducted a preliminary investigation of the magnitude-dependent errors in positions derived from POSS I plates, concluding that the effects are significant and will adversely affect the planned POSS I–POSS II proper motions, for instance. The Schmidt plate data analyzed by Lu et al. had not been corrected with the coma term derived by Morrison et al. (1996), and further work is needed in this area in quantifying the plate-to-plate component of the Schmidt plate magnitude equation.

To the extent that this component is significant, we suggest that the SPM provides a sufficiently deep and dense

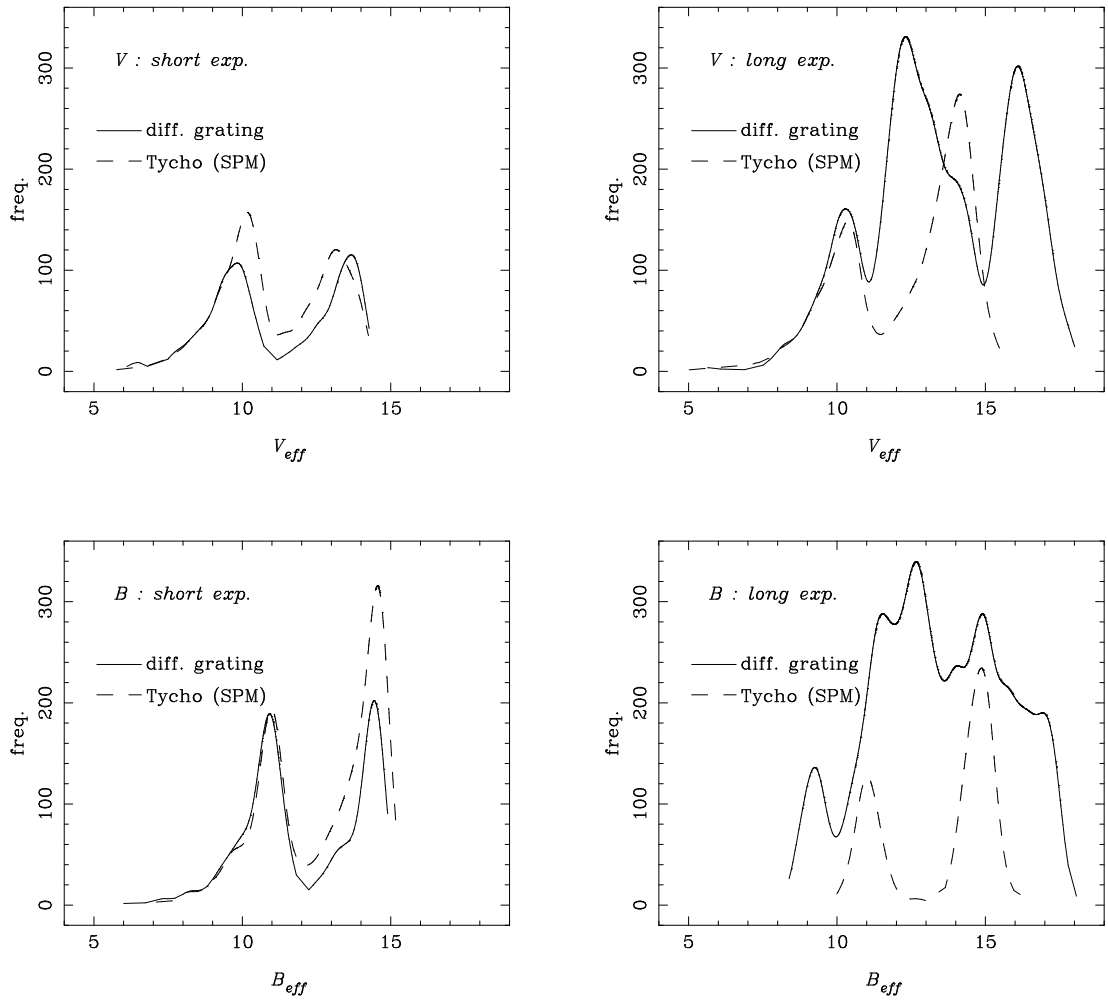


FIG. 12.—Effective magnitude distributions of SPM-measured Tycho stars and of anonymous central/grating-order pairs used in the differential-grating method of magnitude equation correction. The distributions shown are for a representative pair of second-epoch plates (No. 598) near the SGP. The top panels correspond to the visual plate, and the bottom panels correspond to the blue plate. The distributions in the short and long exposures are shown in the left and right panels, respectively.

reference catalog with which *individual* Schmidt survey plates may be directly calibrated.

We wish to thank the many former and present members of Cesco Observatory, Universidad Nacional de San Juan, and Yale Southern Observatory who have contributed to the SPM program over the years. We are also pleased to acknowledge the aid and advice of Arnold Klemola, Burton Jones, and Robert Hanson of Lick Observatory, whose experience with the Northern Proper Motion Program made our job that much easier. We also wish to thank Harvey MacGillivray and Daryl Yentis for providing portions of the UK Schmidt/COSMOS Object Catalog, which is invaluable to our input catalog preparation. And we are grateful to the *Hipparcos* science team for the arrangements by which we were afforded early access to the superb *Hipparcos* data. This research has made use of the SIMBAD database, operated at CDS, Strasbourg, France. The SPM Program is supported by grants from the National Science Foundation.

## REFERENCES

Bastian, U., Roeser, S., & Yagudin, L. I. 1993, PPM Star Catalogue, vol. III–IV (Heidelberg: Spektrum Akad.)
Bucciarelli, B., Sturch, C. R., Lasker, B. M., Lattanzi, M. G., Girard, T. M., Platais, I., & van Altena, W. F. 1995, in IAU Symp. 166, Astronomical and Astrophysical Objectives of Sub-Milliarcsecond Optical Astrometry, ed. E. Høg & P. K. Seidelmann (Dordrecht: Kluwer), 375
Dinescu, D. I., Girard, T. M., van Altena, W. F., Yang, T.-G., & Lee, Y.-W. 1996, AJ, 111, 1205
Eichhorn, H. 1956, AJ, 61, 3
ESAB. 1997, The Hipparcos and Tycho Catalogues (ESA SP-1200) (Noordwijk: ESA)
Jefferys, W. H. 1962, AJ, 67, 532
Klemola, A. R., Jones, B. F., & Hanson, R. B. 1987, AJ, 94, 501
Kozhurina-Platais, V., Girard, T. M., Platais, I., van Altena, W. F., Ianna, P. A., & Cannon, R. D. 1995, AJ, 109, 672
Lee, J.-F., & van Altena, W. F. 1983, AJ, 88, 1683

Lindegren, L., & Kovalevsky, J. 1995, A&A, 304, 189
Lu, C.-L., Platais, I., Girard, T. M., Kozhurina-Platais, V., van Altena, W. F., López, C. E., & Monet, D. G. 1997, in IAU Symp. 179, New Horizons from Multi-Wavelength Sky Surveys, ed. B. McLean (Boston: Kluwer), in press
Morrison, J. E., Röser, S., Lasker, B. M., Smart, R. L., & Taff, L. G. 1996, AJ, 111, 1405
Platais, I., et al. 1992, in ESO Conf. Workshop Proc. 43, Astronomy from Large Databases II, ed. A. Heck & F. Murtagh (Garching: ESO), 455
Platais, I., Girard, T. M., van Altena, W. F., & López, C. E. 1993, in Workshop on Databases for Galactic Structure, ed. A. G. D. Philip, B. Hauck, & A. R. Upgren (Schenectady: L. Davis), 153
Platais, I., Girard, T. M., van Altena, W. F., Ma, W. Z., Lindegren, L., Crifo, F., & Jahreiss, H. 1995, A&A, 304, 141
Platais, I., et al. 1998a, in preparation
Platais, I., Kozhurina-Platais, V., Girard, T. M., van Altena, W. F., López, C. E., MacGillivray, H. T., Yentis, D. J., Kovalevsky, J., & Lindegren, L. 1998b, A&A, in press
Schlesinger, F., & Hudson, C. J. 1914, Publ. Allegheny Obs., 3, 59